BJP BRITISH JOURNAL OF PHARMACOLOGY

BPS BRITISH PHARMACOLOGICAL SOCIETY

British Journal of Pharmacology (2010), 159, 77–92

0007-1188/09
www.brjpharmacol.org

THEMED SECTION: QT SAFETY

RESEARCH PAPER

Dog left ventricular midmyocardial myocytes for assessment of drug-induced delayed repolarization: short-term variability and proarrhythmic potential

Najah Abi-Gerges, Jean-Pierre Valentin and Chris E Pollard

Safety Pharmacology Department, Safety Assessment UK, AstraZeneca R&D, Alderley Park, Macclesfield, Cheshire, UK

Background and purpose: Evaluation of the potential for delayed ventricular repolarization and proarrhythmia by new drugs is essential. We investigated if dog left ventricular midmyocardial myocytes (LVMMs) that can be used as a preclinical model to assess drug effects on action potential duration (APD) and whether in these cells, short-term variability (STV) or triangulation could predict proarrhythmic potential.
Experimental approach: Beagle LVMMs and Purkinje fibres (PFs) were used to record APs. Effects of six reference drugs were assessed on APD at 50% (APD_{50}) and 90% (APD_{90}) of repolarization, STV(APD), triangulation (ratio APD_{90}/APD_{50}) and incidence of early afterdepolarizations (EADs) at 1 and 0.5 Hz.
Key results: LVMMs provided stable recordings of AP, which were not affected by four sequential additions of dimethyl sulphoxide. Effects of dofetilide, d-sotalol, cisapride, pinacidil and diltiazem, but not of terfenadine, on APD in LVMMs were found to be comparable with those recorded in PFs. LVMMs, but not PFs, exhibited a proarrhythmic response to I_{Kr} blockers. Incidence of EADs was not related to differences in AP prolongation or triangulation, but corresponded to beat-to-beat variability of repolarization, here quantified as STV of APD.
Conclusions and implications: LVMMs provide a suitable preclinical model to assess the effects of new drugs on APD and also yield additional information about putative indicators of proarrhythmia that add value to an integrated QT/TdP risk assessment. Our findings support the concept that increased STV(APD) may predict drug-induced proarrhythmia.
British Journal of Pharmacology (2010) **159,** 77–92; doi:10.1111/j.1476-5381.2009.00338.x; published online 6 August 2009

This article is part of a themed section on QT safety. To view this issue visit http://www3.interscience.wiley.com/journal/121548564/issueyear?year=2010

Keywords: left ventricular midmyocardial myocytes; Purkinje fibres; action potential duration; triangulation; beat-to-beat variability of repolarization

Abbreviations: AP, action potential; APD, AP duration; APD_{50} and APD_{90}, duration of the AP at 50 and 90% repolarization; BVR, beat-to-beat variability of repolarization; CAVB, chronic AV block; EADs, early afterdepolarizations; EFPTC, effective free therapeutic plasma concentration; IC_{50}, molar concentration of a drug producing 50% inhibition; I_{Ca}, inward cardiac Ca^{2+} current; I_{KATP}, adenosine triphosphate (ATP)-sensitive cardiac K^+ current; I_{Kr}, rapid delayed rectifier cardiac K^+ current; I_{Ks}, slow delayed rectifier cardiac K^+ current; LVMMs, left ventricular midmyocardial myocytes; MAPD, monophasic APD; PFs, Purkinje fibres; STV(APD), short-term variability of APD; STV, short-term variability; TRIaD, triangulation, reverse frequency-dependence, instability and dispersion of the AP

Introduction

Numerous cardiovascular and non-cardiovascular drugs causing the polymorphic ventricular tachycardia, Torsades de Pointes (TdP), have been a major focus of regulatory authorities and the pharmaceutical industry since the mid-1990s

Correspondence: Dr Najah Abi-Gerges, AstraZeneca, 19B70, Mereside, Alderley Park, Macclesfield, Cheshire, SK10 4TG, UK. E-mail: najah.abigerges@astrazeneca.com
Received 6 January 2009; revised 10 February 2009; accepted 2 April 2009

(Fenichel *et al.*, 2004; Bass *et al.*, 2007). This concern has led to the adoption of International Conference on Harmonization (ICH) S7B and ICH E14 guidance documents (Anon, 2005a,b), both of which rely on prolongation of the QT interval as a biomarker to predict the risk that a drug may produce TdP. Therefore, evaluation of the effects of new compounds on cardiac action potential duration (APD) is regarded as an essential assessment in the pharmaceutical industry. Recent data, however, suggest that a prolonged QT interval cannot reliably predict the torsadogenic risk of a drug (Thomsen *et al.*, 2006; Antzelevitch, 2007). As a result, over the last few years, there has been a shift in emphasis with respect to assessing the effects of a new drug on cardiac repolarization and its proarrhythmic potential. Specifically, rather than simply assessing the QT interval prolongation risk, effort is being expended looking for other preclinical markers that will predict proarrhythmic risk. Because it was found that the incidence of TdP correlated well with the degree of 'beat-to-beat' variability of repolarization (BVR), quantified as short-term variability (STV), STV has been proposed as a potentially better predictor for torsadogenic risk than QT interval prolongation (Thomsen *et al.*, 2004; 2006). Additionally, an increase in AP triangulation, an important component of TRIaD (triangulation, reverse frequency-dependence, instability and dispersion of the AP), is thought to be a sensitive indicator of increased torsadogenic risk (Hondeghem and Hoffmann, 2003; Hondeghem *et al.*, 2003; Hondeghem, 2007).

The cardiac Purkinje fibres (PFs) are commonly used to evaluate the effects of new drugs on APD (Anon, 2000; 2005a). Although dog PFs have been shown to be suitable for this purpose (Gintant *et al.*, 2001; Lu *et al.*, 2001; Abi-Gerges *et al.*, 2004; Champeroux *et al.*, 2005), throughput is low, and animal demand is high. Additionally, multicellular *in vitro* preparations, like the PFs, may present a significant barrier to the diffusion of drugs to the cardiac cells from which intracellular APs are being recorded (Cavero *et al.*, 1999). The use of single isolated ventricular myocytes may be one way of avoiding this problem by ensuring rapid access of drugs to the recorded cell. Although recent studies comparing the utility of preclinical models (including PF and papillary muscle) to detect drug-induced delay in ventricular repolarization have not included ventricular myocytes in their assessment (Omata *et al.*, 2005; Hanson *et al.*, 2006), the use of guinea pig ventricular myocytes as a preclinical model for testing drug-induced changes in APD has been investigated (Davie *et al.*, 2004; Terrar *et al.*, 2007). Even though Terrar *et al.* (2007) showed that guinea pig myocytes provide a suitable alternative model to PFs in tests for drug effects on APD, it is unclear to what extent guinea pig electrophysiology resembles that of man.

As the distribution of ion channel proteins and ionic currents that determine the AP shape and duration are strikingly similar in dog and human ventricles (Szabo *et al.*, 2005), the beagle dog is a commonly used preclinical species to test the effects of new drugs on cardiac repolarization (Gralinski, 2003), and repolarization of the midmyocardial ventricyular myocytes usually determines the end of the T-wave (Antzelevitch, 2007), which means that data from these myocytes may better relate to QT measurements, the main motivation of this investigation was to determine if left ventricular midmyocardial myocytes (LVMMs) from beagle dogs could be used as a preclinical model to assess drug effects on AP repolarization. In particular, we set out to: (i) test the effects of six reference drugs (four of them with a known TdP risk) on APD; (ii) determine what temporal STV(APD), triangulation and incidence of early afterdepolarizations (EADs) data they yield in the presence of the validation set; and (iii) compare data from LVMMs to those obtained in PFs from beagle dogs.

Methods

Isolations of LVMMs and PFs

Alderley Park female beagle dogs were used (weight 7.55–16.75 kg; age 9–29 months). They were maintained in accordance with the Guide for The UK Home Office Code and Practice for the Housing and Care of Animals used in Scientific Procedures. The procedures were authorized under a project licence granted under the Animals (Scientific Procedures) Act 1986.

Electrophysiological experiments were performed on isolated LVMMs and intact PFs. Midmyocardial myocytes were isolated enzymatically from the left ventricular midmyocardium of the heart as previously described (Volders *et al.*, 1998). Briefly, hearts were excised from anesthetized dogs (45 $mg \cdot kg^{-1}$ pentobarbitone) and washed in an O_2-gassed, Ca^{2+}-free, standard myocyte Tyrode solution (see below for composition) at approximately 4°C. A cannula was quickly inserted into and sutured to the left anterior descending artery under continuous perfusion with the same Tyrode solution. Subsequent perfusion was done at 37°C with O_2-gassed, Ca^{2+}-free, standard myocyte Tyrode solution for 5–10 min and then for 18–22 min with the same solution plus collagenase. Collagenase was then washed out with O_2-gassed, 0.2 mM Ca^{2+}-standard myocyte Tyrode solution for 5–8 min. Finally, LVMMs were isolated by careful harvesting of the middle third of the transmural wall of the perfused wedge and were stored at room temperature in standard myocyte Tyrode solution. A sample of the LVMM suspension was transferred to a heated chamber (HW-30 Temperature Controller, Dagan Corporation, Minnesota, USA) mounted on the stage of an inverted microscope (TE 2000-U Eclipse, Nikon Europe B.V., The Netherlands) and continuously superfused with standard myocyte Tyrode solution at a rate of 3 $mL \cdot min^{-1}$ at 37 ± 0.5°C, using a pressure-driven drug application device (ALA Scientific Instruments, NY, USA). Only quiescent rod-shaped cells with clear cross-striations were used for the experiments.

To isolate intact PFs, the experimental approach used is similar to that in our recent study (Abi-Gerges *et al.*, 2004). Briefly, the heart was excised and placed in a standard PF Tyrode solution (see below), maintained at 4°C and previously saturated with a 95% O_2/5% CO_2 mixture. Free running PFs were isolated from the left ventricle of the heart and placed in a custom-made glass-recording chamber and perfused with 95% O_2/5% CO_2-gassed standard PF Tyrode solution at a rate of 5 $mL \cdot min^{-1}$ using a peristaltic pump (Gilson Minipuls 3, Gilson Inc., Villiers-le-Bel, France). The temperature in the recording chamber was maintained at 37.4 ± 0.1°C.

Table 1 Nominal concentrations tested in dog PFs and LVMMs and ratio to clinical concentrations

Drug	*EFTPC$_{max}$ (μM)*[a,b]	*Concentrations tested (μM)*						*Concentrations as multiple of EFTPC$_{max}$*					
Cisapride	0.0049	0.01	0.1	1	10			2	20	204	2040		
Dofetilide	0.002	0.001	0.01	0.1	1			0.5	5	50	500		
Terfenadine	0.009	0.01	0.1	1	10			1.1	11	111	1111		
Diltiazem	0.122	1	3	10	30			8	24	82	246		
Pinacidil[c]	1	0.01	0.1	1	3	10	30	0.01	0.1	1	3	10	30
d-sotalol	2–14	1	10	30	100			0.06	0.6	2	6.8		
dl-sotalol[d]	2–14	1	10	30	100			0.06	0.6	2	6.8		
DMSO 0.1%	N/A	N/A	N/A	N/A	N/A			N/A	N/A	N/A	N/A		

[a]Redfern *et al.* (2003).
[b]Lawrence *et al.* (2006).
[c]Concentration range 0.01–3 μM of pinacidil was tested in Purkinje fibre preparation.
[d]dl-Sotalol was assessed in LVMMs.
DMSO, dimethylsulphoxide; EFTPC$_{max}$, maximum effective free therapeutic plasma concentration; LVMMs, left ventricular midmyocardial myocytes; N/A, not applicable; PFs, Purkinje fibres.

Solutions and drugs

The standard myocyte Tyrode solution contained (in mM): NaCl 145, KCl 4, $CaCl_2$ 1.8, $MgCl_2$ 1, glucose 11.1 and HEPES 10, pH 7.4 with NaOH. For myocyte isolation, collagenase (1.1 mg·mL^{-1}; type A, Roche, Germany) was used in the presence of BSA (1 mg·mL^{-1}). The standard PF Tyrode solution contained (in mM): NaCl 118, KCl 4, $MgCl_2$ 1, $CaCl_2$ 1.8, $NaHCO_3$ 31, NaH_2PO_4 1.8, glucose 11 and pH 7.4 with NaOH.

Drugs selected for this investigation consist of two class III antiarrhythmic drugs [dofetilide and d-sotalol; selective blockers of I_{Kr} (rapid delayed rectifier cardiac K^+ current)], two multiple ion channel blockers (terfenadine and cisapride; I_{Kr} inhibitors, but also with actions on other cardiac ion channels), an I_{KATP} (ATP-sensitive cardiac K^+ current) opener (pinacidil) and an $I_{Ca,L}$ inhibitor (diltiazem). Additionally, dl-sotalol (racemic mixture of sotalol; an I_{Kr} inhibitor but also a β-adrenoceptor antagonist) was tested in LVMMs and compared with the effects of d-sotalol. Dofetilide and cisapride were purchased from Apin Chemicals Ltd (Abingdon, UK) and AstraZeneca Mölndal, Sweden provided d-sotalol. All the other drugs and chemicals were purchased from Sigma-Aldrich Company Ltd (Poole, UK) and Fluka (York, UK). On each experimental day, each drug was formulated as a dimethylsulphoxide (DMSO) stock that was then serially diluted in DMSO to give three further DMSO stocks (in mM). Finally, each of these stocks was diluted 1000× in standard Tyrode solution to give the final test concentrations indicated in Table 1.

Electrophysiological measurements

Left ventricular midmyocardial myocyte and PF transmembrane potentials were recorded with glass micropipettes filled with 3 M KCl, with tip resistances between 20–40 and 10–18 MΩ respectively. The micropipette was connected to the headstage of a MultiClamp 700A amplifier (Axon Instruments Inc., Union City, CA, USA). AP signals from LVMMs and PFs were acquired using Clampex 9.2 (Axon Instruments Inc., Union City, CA, USA) and AP software (Notocord HEM 3.4 or 3.5; Notocord Systems S.A., Croissy Sur Seine, France), respectively, at pacing frequencies of 1 and 0.5 Hz. Additional offline analysis, using validated macros, was carried out, and APD was measured (in both preparations) at 50 and 90% repolarization (APD_{50} and APD_{90}). Data for each experimental condition were the mean of 15 APDs at 0.5 Hz or 30 APDs at 1 Hz. The ratio of APD_{90}/APD_{50} was analysed to describe AP triangulation (Milberg *et al.*, 2004), and temporal BVR was quantified as STV from APD Poincaré plots over a period of 30 s, which was calculated as $\Sigma|APD_{n+1} - APD_n|/[n_{beats} \times \sqrt{2}]$ (Thomsen *et al.*, 2004). APD, STV(APD) and triangulation for each experimental condition were either collected once steady state was achieved in cells without EADs or measured just before first EAD in cells with EADs. An EAD was identified as abnormal depolarization during phase 2 or phase 3 and caused by an increase in the frequency of abortive APs before normal repolarization is completed.

Experimental protocol

A stabilization period in both preparations was allowed before the experimental protocol was carried out. Following the stabilization period, data acquisition was commenced, providing APs were typical of those observed in PFs (Abi-Gerges *et al.*, 2004) and dog LVMMs (Volders *et al.*, 2003; Thomsen *et al.*, 2004; Stengl *et al.*, 2006). AP stability was assessed again in the first 5–10 min of recording in the standard Tyrode solution at a pacing frequency of 1 Hz. Rate adaptation was investigated by changing the pacing frequency in the following sequence; 1, 0.5 and 1 Hz, ensuring steady state was achieved at each frequency prior to changing to the next rate. Following exposure to the standard Tyrode solution, the same sequence was repeated during perfusion of the same preparation with standard Tyrode solution containing vehicle (0.1% DMSO), then with four ascending concentrations of drug to form a cumulative concentration-effect curve over the nominal concentration range shown in Table 1. Experimental conditions (perfusate solution or pacing frequency) were only changed once any alteration in AP parameters evoked by the prevailing conditions was at steady state. If, following a change in the solution being perfused, there did not appear to have been an effect on AP parameters at 1 Hz pacing frequency, a minimum of 10 min in PFs and 2 min in LVMMs was allowed to elapse before changing to 0.5 Hz pacing frequency.

Statistics
As each dog heart yielded many LVMMs, it was possible to study more than one drug following each isolation. However, it was not necessarily possible to complete all the testing required on a drug in a single isolation. Thus, a given drug may have been tested on six LVMMs, but four came from one dog, and two from another dog. In this circumstance, the data are considered $n = 6$, and in the 'Results' section, the replicates information is expressed as $n = 6$ cells (two dogs). On the other hand, when expressed as $n = 8$ fibres (eight dogs), the replicates information means that a given drug may have been tested on eight PFs that came from eight different dogs. Drug effects were quantified relative to the data collected during the perfusion of vehicle. Results are expressed as mean ± SEM. Differences were tested for statistical significance using the paired (two sample for means; same cardiac preparation) and unpaired (two sample assuming unequal variances; one preparation *vs*. another) Student's *t*-test. A value of $P < 0.05$ was considered significant.

Results

Stability of AP recordings in LVMMs and time-control data for APD
The stability of AP recordings over time in LVMMs was investigated by measuring APD in control conditions at a pacing frequency of 1 Hz for up to 32 min. APDs recorded over this period were stable (Figure 1A and B). Moreover, STV(APD) or APD_{90}/APD_{50} ratio did not significantly change over time (Figure 1C and D).

Before constructing concentration-effect curves for the effect of ion channel modulators on APD, we first established time-control data using four additions of vehicle solution (0.1% DMSO) to mimic an experiment with an active drug. At a pacing frequency of either 1 or 0.5 Hz, neither the 1st, 2nd, 3rd or 4th vehicle addition significantly affected APD_{90} in LVMMs or PFs relative to baseline values of vehicle solution (Figure 1E and F). The same was true for APD_{50} (data not shown). Thus, beagle LVMMs provide very stable recordings of AP under the experimental conditions of this study, and sequential DMSO additions do not significantly affect AP parameters, thus illustrating they can be used to generate meaningful four-point concentration-effect curves.

Effects of reference drugs on APD in LVMMs and PFs
Dofetilide and d-sotalol (Carmeliet, 1985; Gwilt *et al*., 1991; Obreztchikova *et al*., 2003; Thomsen *et al*., 2004), cisapride and terfenadine (Ming and Nordin, 1995; Davie *et al*., 2004; Li *et al*., 2006; Hanson *et al*., 2006), pinacidil and diltiazem (Balati *et al*., 1998; Gintant *et al*., 2001; Lu *et al*., 2007) are drugs frequently used as reference drugs that are expected to increase, have biphasic effects and decrease APD respectively. APD responses to these reference drugs in LVMMs were found to be comparable with those found with PFs, with exception of terfenadine (Tables 2–5). Although both dofetilide and d-sotalol caused AP prolongation, greater increases in APD were observed in PFs compared with LVMMs (Tables 2 and 5). d-Sotalol-induced increases in APD were greater at 30 and 100 μM compared with dl-sotalol. Additionally, APD_{90} increases at 1 Hz pacing frequency after exposure to dofetilide (1 μM), which are shown in Figure 3B, suggest that drug effects on APD are largely independent of isolations in LVMMs.

Cisapride caused biphasic effects on APD in both preparations (Tables 3 and 5). Although the maximum increase in APD_{90} was seen at 1 μM in PFs during pacing frequencies of 1 and 0.5 Hz, maximum APD_{90} increases in LVMMs were seen at 0.1 μM during 1 Hz and 1 μM during 0.5 Hz (Table 3). Moreover, as reported by others (Gintant *et al*., 2001; Terrar *et al*., 2007), terfenadine did not significantly affect APD in PFs at either pacing frequency, except for a small, but statistically significant decrease in APD_{50} at 10 μM (Tables 3 and 5). This absence of effect in PFs was not due to a lack of exposure of the recorded cell to terfenadine, as this drug caused a concentration-dependent decrease in maximum upstroke velocity (relative to vehicle, % change value at 1 Hz was –22.8 ± 9.3% at 10 μM [$n = 7$ fibres (seven dogs); $P < 0.05$ vs. vehicle]. This decrease in maximum upstroke velocity was less marked at 0.5 Hz (% change value at 10 μM was –7.2 ± 4.1%; $P > 0.05$ vs. vehicle and values at 1 Hz). In contrast, in LVMMs, while 0.01 μM terfenadine did not affect APD, at 0.1 μM, it induced a small but significant increase in APD, and at 1 and 10 μM, a significant decrease in APD [$n = 8$–10 cells (two dogs)] (Tables 3 and 5). No reverse frequency-dependent APD effect was seen with terfenadine in either preparation.

Pinacidil caused a concentration-dependent decrease in APD. Although higher concentrations were needed to shorten the AP in LVMMs, APD decrease in both preparations was not affected by a low pacing frequency, and the percentage decrease in APD_{50} was greater than that on APD_{90} at 1 and 3 μM in PFs only (Tables 4 and 5). Additionally, concentration-dependent shortening of the AP was seen after exposure to diltiazem. Although the effects of diltiazem on APD_{50} were greater than those on APD_{90} in PFs, effects on APD in LVMMs were broadly similar, and decreases in APD in both preparations were not different during low pacing frequency (Tables 4 and 5).

Effects of reference drugs on STV(APD) and triangulation in LVMMs and PFs
We sought to determine what temporal BVR and triangulation information LVMMs and PFs yield in the presence of the reference drugs.

Dofetilide and d-sotalol. In contrast to LVMMs (Figure 3C and D), APD in PFs did not vary in consecutive beats in the presence of 1 μM dofetilide (Figure 3A). Grouped average data show a marked increase in $STV(APD_{90})$ in LVMMs, with increasing concentrations of either dofetlide or d-sotalol at both pacing frequencies, although no significant changes in $STV(APD_{90})$ were seen in PFs at either pacing frequency (Table 2). Similar findings were observed for $STV(APD_{50})$ with dofetilide (Figure 3C and D) and d-sotalol in both preparations (average data not shown). Even though dofetilide and d-sotalol increased STV(APD) in all LVMMs, dofetilide elicited EADs only in four out of six cells (two cells at 0.1 μM at 1 Hz; two cells at 0.1 μM and 1 μM at 0.5 Hz), and d-sotalol-induced

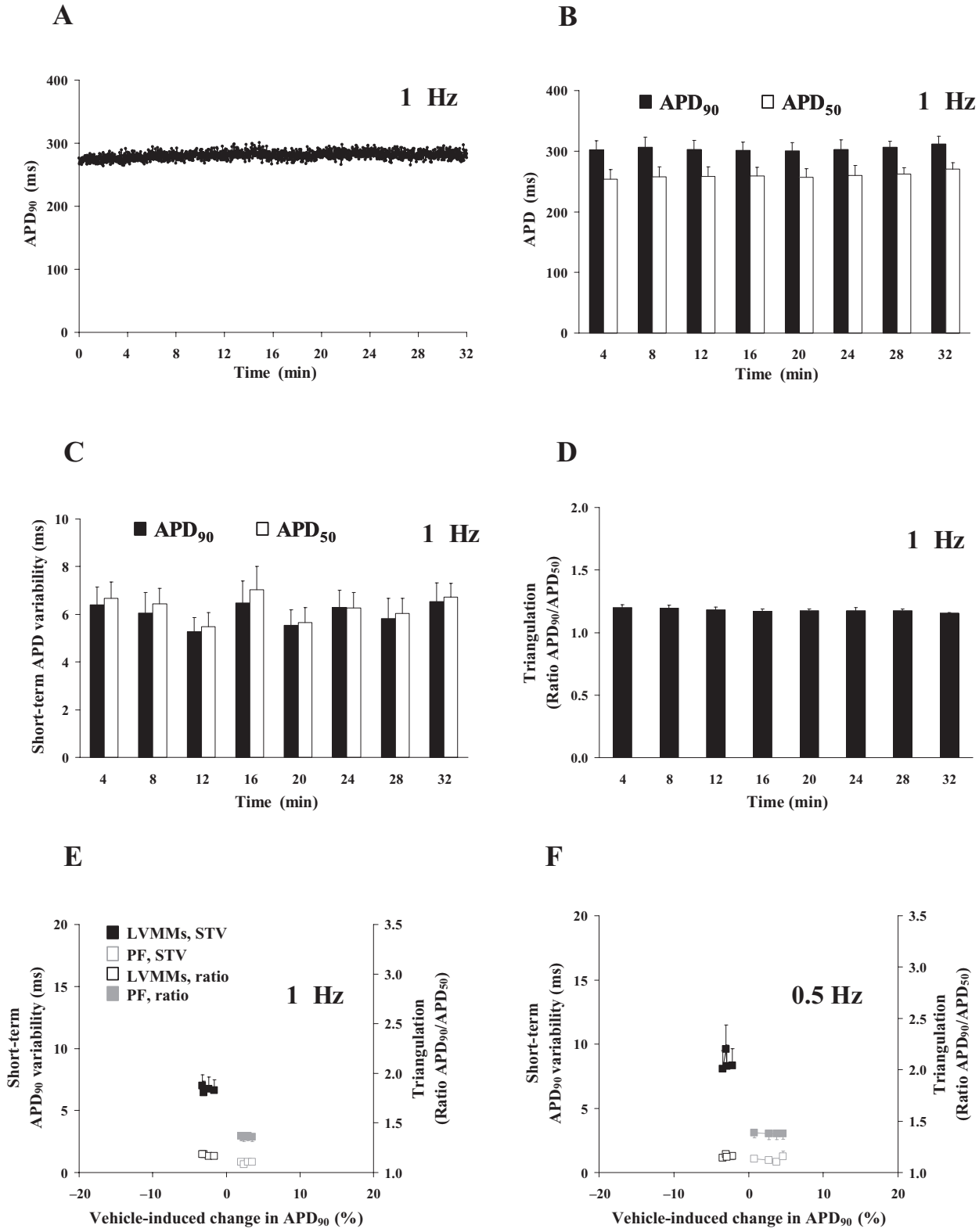

Figure 1 Stability of AP recordings over time in beagle LVMMs. (A) APD_{90} was measured in standard myocyte Tyrode solution from APs stimulated at a pacing frequency of 1 Hz for 32 min. (B, C and D) Grouped data show that APD, STV(APD) and triangulation (ratio APD_{90}/APD_{50}) were not changed over a period of 32 min [n = 4–10 cells (five dogs); $P > 0.05$ vs. values from 4 min period]. Effects of four additions of vehicle (0.1% DMSO; to mimic an experiment with an active drug) on STV(APD_{90}) and triangulation as a function of change in APD_{90} in LVMMs [n = 8–9 cells (two dogs)] and PFs [n = 8 fibres (eight dogs)] at pacing frequencies of 1 (E) and 0.5 Hz (F). Note that the effects of vehicle on STV(APD_{90}) and triangulation are plotted on a separate y axis. AP, action potential; APD, action potential duration; APD_{50} and APD_{90}, duration of the AP at 50% and 90% repolarization; DMSO, dimethylsulphoxide; LVMMs, left ventricular midmyocardial myocytes; PFs, Purkinje fibres; STV, short-term variability.

Table 2 Effects of dofetilide, d-sotalol and dl-sotalol on STV(APD_{90}) and triangulation (ratio of APD_{90}/APD_{50}) as a function of change in APD_{90} in dog PFs and LVMMs

Drug	*Preparation*	*Animals*	n	*Pacing*	*Parameter*	*Baseline*	*Nominal concentrations tested*			
Dofetilide							0.001 μM	0.01 μM	0.1 μM	1 μM
	PF	7	7	1.0 Hz	APD_{90} (ms)	292 ± 8	10 ± 5%*	44 ± 3%*♣	76 ± 6%*	91 ± 6%*♣
					STV(APD_{90}) (ms)	0.5 ± 0.08♣	0.4 ± 0.03♣	0.5 ± 0.1♣	0.7 ± 0.3♣	0.6 ± 1♣
					Triangulation	1.37 ± 0.02♣	1.35 ± 0.02♣	1.37 ± 0.03♣	1.38 ± 0.03♣	1.35 ± 0.02♣
				0.5 Hz	APD_{90} (ms)	328 ± 12	10 ± 5%#	57 ± 4%#$♣	105 ± 9%#$♣	134 ± 12%#$
					STV(APD_{90}) (ms)	0.4 ± 0.04♣	0.4 ± 0.06♣	0.5 ± 0.07♣	0.8 ± 0.1♣	0.8 ± 0.1♣
					Triangulation	1.36 ± 0.02♣	1.35 ± 0.02♣	1.39 ± 0.04♣	1.39 ± 0.03♣	1.38 ± 0.03♣
	LVMM	4–6	2	1.0 Hz	APD_{90} (ms)	377 ± 18	0.4 ± 2%	15 ± 6%*	46 ± 12%*	37 ± 12%*
					STV(APD_{90}) (ms)	12 ± 2	11 ± 2	27 ± 13	51 ± 15*	33 ± 5*
					Triangulation	1.19 ± 0.03	1.18 ± 0.02	1.17 ± 0.02	1.19 ± 0.02	1.16 ± 0.02
				0.5 Hz	APD_{90} (ms)	436 ± 25	−3 ± 2%	11 ± 5%*	36 ± 13%*	74 ± 20%*
					STV(APD_{90}) (ms)	16 ± 4	15 ± 3	21 ± 5	38 ± 8*	92 ± 19*$
					Triangulation	1.16 ± 0.03	1.15 ± 0.02	1.13 ± 0.02	1.13 ± 0.02	1.11 ± 0.01
d-sotalol							1 μM	10 μM	30 μM	100 μM
	PF	4	4	1.0 Hz	APD_{90} (ms)	270 ± 8	0.5 ± 0.7%	16 ± 3%*	36 ± 7%#♣	59 ± 12%#♣
					STV(APD_{90}) (ms)	0.4 ± 0.03♣	0.5 ± 0.15♣	0.5 ± 0.16♣	0.8 ± 0.2♣	1 ± 0.3♣
					Triangulation	1.41 ± 0.03♣	1.40 ± 0.05	1.39 ± 0.05	1.40 ± 0.05	1.41 ± 0.05
				0.5 Hz	APD_{90} (ms)	295 ± 10	0.5 ± 0.3%	20 ± 6%*	42 ± 9%*	77 ± 19%*
					STV(APD_{90}) (ms)	0.7 ± 0.2♣	0.8 ± 0.3♣	0.6 ± 0.2♣	0.6 ± 0.3♣	1.2 ± 0.3♣
					Triangulation	1.41 ± 0.03	1.38 ± 0.04♣	1.37 ± 0.04♣	1.38 ± 0.04	1.40 ± 0.04♣
	LVMM	4	3	1.0 Hz	APD_{90} (ms)	364 ± 18	−4 ± 2%	12 ± 3%*	14 ± 4%*	28 ± 3%#
					STV(APD_{90}) (ms)	8 ± 1	7 ± 1	13 ± 1*	13 ± 1*	20 ± 2#
					Triangulation	1.20 ± 0.04	1.18 ± 0.03	1.21 ± 0.05	1.21 ± 0.04	1.22 ± 0.06
				0.5 Hz	APD_{90} (ms)	427 ± 27	−9 ± 4%	2 ± 1%	22 ± 7%*	37 ± 6%#
					STV(APD_{90}) (ms)	12 ± 1	10 ± 2	13 ± 3	22 ± 4*$	33 ± 7*
					Triangulation	1.26 ± 0.1	1.18 ± 0.02	1.18 ± 0.03	1.19 ± 0.05	1.16 ± 0.05
dl-sotalol							1 μM	10 μM	30 μM	100 μM
	LVMM	7	1	1.0 Hz	APD_{90} (ms)	348 ± 12	−3 ± 1%	4 ± 3%	5 ± 3%	15 ± 5%*
					STV(APD_{90}) (ms)	7 ± 1	6 ± 1	8 ± 2	7 ± 1	12 ± 4
					Triangulation	1.30 ± 0.06	1.26 ± 0.05	1.25 ± 0.04	1.24 ± 0.04	1.24 ± 0.04
				0.5 Hz	APD_{90} (ms)	400 ± 12	−5 ± 2%	−1 ± 2%	4 ± 4%	18 ± 9%*
					STV(APD_{90}) (ms)	9 ± 2	8 ± 2	10 ± 1	12 ± 2	13 ± 2
					Triangulation	1.30 ± 0.07	1.26 ± 0.05	1.23 ± 0.05	1.23 ± 0.04	1.22 ± 0.05

Changes in APD_{90}, STV(APD_{90}) and triangulation were measured in (i) dofetilide- and d-sotalol-treated cells with (before first EAD) and without (once steady state was achieved) EADs; and (ii) dl-sotalol-treated cells once steady state was achieved.
*$P < 0.05$ and #$P < 0.01$ versus values from vehicle; $$P < 0.05$ versus values at 1.0 Hz; ♣$P < 0.05$ versus values in LVMMs at 1.0 Hz; ♣$P < 0.05$ versus values in LVMMs at 0.5 Hz.
APD, action potential duration; APD_{50} and APD_{90}, duration of the AP at 50 and 90% repolarization; EADs, early afterdepolarizations; LVMMs, left ventricular midmyocardial myocytes; PFs, Purkinje fibres; STV, short-term variability.

EADs were seen in two out of four cells (two cells at 100 μM at 0.5 Hz). However, no EADs were seen in any dofetilide- or d-sotalol-treated PFs. Compared with the proarrhythmic potential of d-sotalol, the racemic form, dl-sotalol, exhibits dual actions that account for its overall antiarrhythmic properties and therapeutic utility (Singh, 1999). Grouped average data show no significant increase in STV(APD_{90}) with increasing dl-sotalol concentrations at 1 and 0.5 Hz (Table 2). Similar findings were observed for STV(APD_{50}) (data not shown). None of the myocytes demonstrated EADs in presence of dl-sotalol. Furthermore, no triangular pattern of APD prolongation was evoked by dofetilide, d-sotalol or dl-sotalol in either PFs or LVMMs (Table 2).

Cisapride and terfenadine. A concentration-dependent biphasic effect on STV(APD_{90}) was observed in LVMMs, but not in PFs, with increasing cisapride concentrations at 1 and 0.5 Hz (Table 3). The maximum increase in STV(APD_{90}) occurred at 0.1 and 1 μM during 1 Hz and 0.5 Hz respectively (Table 3). This increase was reversed on 10 μM cisapride application such that STV(APD_{90}) was not significantly different from vehicle values. Similar findings were seen for STV(APD_{50}) in both preparations (data not shown). Three out of 10 LVMMs showed EADs on cisapride application (two myocytes at 0.1 μM at 1 and 0.5 Hz; one myocyte at 1 μM at 0.5 Hz); however, no EADs were seen in seven PFs treaded with cisapride. Additionally, the ratio of APD_{90}/APD_{50} showed a triangular pattern of APD change for cisapride (Table 3). In PFs, at both pacing frequencies, cisapride caused a concentration-dependent increase in triangulation that became statistically significant at 10 μM, and the increase in triangulation tended not to be different during low pacing frequency (Table 3). In LVMMs, however, a significant increase in triangulation was only seen at the highest concentration during 1 and 0.5 Hz, and the increase in triangulation was not different during low pacing frequency (Table 3).

Terfenadine did not significantly affect STV(APD_{90}) in PFs at either 1 or 0.5 Hz pacing frequency (Table 3). Similar findings were seen for STV(APD_{50}) (data not shown). At steady state in LVMMs (Figure 2B), terfenadine did not induce significant changes in STV(APD_{90}) at 1 Hz (Table 3). Moreover, while 0.01 and 0.1 μM terfenadine did not significantly increase STV(APD_{90}) during 0.5 Hz, higher concentrations caused a decrease that became significant at 10 μM (Table 3). Further-

Table 3 Effects of cisapride and terfenadine on STV(APD_{90}) and triangulation (ratio of APD_{90}/APD_{50}) as a function of change in APD_{90} in dog PFs and LVMMs

Drug	*Preparation*	*Animals*	n	*Pacing*	*Parameter*	*Baseline*	*Nominal concentrations tested*			
Cisapride							0.01 μM	0.1 μM	1 μM	10 μM
	PF	7	7	1.0 Hz	APD_{90} (ms)	349 ± 12	2 ± 1%	12 ± 1%$^{\#\clubsuit}$	26 ± 4%$^{\#}$	2 ± 5%
					STV(APD_{90}) (ms)	1.6 ± 0.5$^{\clubsuit}$	0.8 ± 0.2$^{\clubsuit}$	1.1 ± 0.3$^{\clubsuit}$	1.56 ± 0.8$^{\clubsuit}$	0.8 ± 0.2$^{\clubsuit}$
					Triangulation	1.33 ± 0.07	1.29 ± 0.03	1.33 ± 0.04	1.62 ± 0.14$^{\clubsuit}$	2.18 ± 0.1$^{\#\clubsuit}$
				0.5 Hz	APD_{90} (ms)	378 ± 20	5 ± 4%	19 ± 4%$^{\#\clubsuit}$	51 ± 10%$^{\#\$}$	16 ± 8%$^{\clubsuit}$
					STV(APD_{90}) (ms)	1.2 ± 0.4$^{\clubsuit}$	0.9 ± 0.2$^{\clubsuit}$	1.3 ± 0.5$^{\clubsuit}$	1.4 ± 0.4$^{\clubsuit}$	1.7 ± 0.5$^{\clubsuit}$
					Triangulation	1.30 ± 0.04$^{\clubsuit}$	1.30 ± 0.04$^{\clubsuit}$	1.34 ± 0.03$^{\clubsuit}$	1.52 ± 0.06$^{*\clubsuit}$	1.98 ± 0.10$^{\#\clubsuit}$
	LVMM	4–10	2	1.0 Hz	APD_{90} (ms)	360 ± 15	3 ± 3%	37 ± 11%$^{\#}$	23 ± 5%$^{\#}$	–12 ± 6%
					STV(APD_{90}) (ms)	7 ± 1	8 ± 1	31 ± 13*	10 ± 2	5 ± 1
					Triangulation	1.22 ± 0.04	1.22 ± 0.05	1.28 ± 0.07	1.29 ± 0.07	1.47 ± 0.10*
				0.5 Hz	APD_{90} (ms)	380 ± 19	7 ± 2%*	46 ± 8%$^{\#}$	69 ± 19%$^{*\$}$	–16 ± 6%
					STV(APD_{90}) (ms)	7 ± 2	12 ± 2	26 ± 5*	42 ± 20*	17 ± 9
					Triangulation	1.14 ± 0.01$^{\$}$	1.14 ± 0.01	1.15 ± 0.01	1.22 ± 0.04	1.36 ± 0.09*
Terfenadine							0.01 μM	0.1 μM	1 μM	10 μM
	PF	7	7	1.0 Hz	APD_{90} (ms)	300 ± 18	0.4 ± 0.8%	0.5 ± 1%$^{\clubsuit}$	4 ± 1%$^{\clubsuit}$	1 ± 2%$^{\clubsuit}$
					STV(APD_{90}) (ms)	0.6 ± 0.1$^{\clubsuit}$	0.7 ± 0.1$^{\clubsuit}$	0.8 ± 0.2$^{\clubsuit}$	0.7 ± 0.1$^{\clubsuit}$	0.6 ± 0.1$^{\clubsuit}$
					Triangulation	1.38 ± 0.04$^{\clubsuit}$	1.35 ± 0.03$^{\clubsuit}$	1.38 ± 0.04$^{\clubsuit}$	1.41 ± 0.04$^{\clubsuit}$	1.60 ± 0.09$^{*\clubsuit}$
				0.5 Hz	APD_{90} (ms)	332 ± 25	1 ± 1%	2 ± 0.7%$^{\clubsuit}$	5 ± 2%$^{\clubsuit}$	5 ± 2%$^{\clubsuit}$
					STV(APD_{90}) (ms)	0.6 ± 0.1$^{\clubsuit}$	0.7 ± 0.2$^{\clubsuit}$	0.8 ± 0.1$^{\clubsuit}$	0.8 ± 0.2$^{\clubsuit}$	0.8 ± 0.2$^{\clubsuit}$
					Triangulation	1.42 ± 0.06$^{\clubsuit}$	1.41 ± 0.06$^{\clubsuit}$	1.41 ± 0.06$^{\clubsuit}$	1.44 ± 0.06	1.57 ± 0.09$^{\clubsuit}$
	LVMM	8–10	2	1.0 Hz	APD_{90} (ms)	369 ± 16	–1 ± 1%	5 ± 2%$^{\#}$	–34 ± 6%$^{\#}$	–74 ± 2%$^{\#}$
					STV(APD_{90}) (ms)	8 ± 1	8 ± 1	8 ± 1	10 ± 2	9 ± 5
					Triangulation	1.15 ± 0.01	1.15 ± 0.01	1.17 ± 0.02	1.27 ± 0.04*	1.36 ± 0.05$^{\#}$
				0.5 Hz	APD_{90} (ms)	424 ± 25	–0.7 ± 1%	6 ± 2%$^{\#}$	–17 ± 6%$^{*\$}$	–67 ± 3%$^{\#}$
					STV(APD_{90}) (ms)	10 ± 2	15 ± 5	15 ± 5	6 ± 2	3 ± 1$^{\#}$
					Triangulation	1.15 ± 0.01	1.15 ± 0.01	1.15 ± 0.01	1.20 ± 0.04	1.36 ± 0.04$^{\#}$

Changes in APD_{90}, STV(APD_{90}) and triangulation were measured in (i) cisapride-treated cells with (before first EAD) and without (once steady state was achieved) EADs; and (ii) terfenadine-treated cells and PFs once steady state was achieved.
$^{*}P < 0.05$ and $^{\#}P < 0.01$ versus values from vehicle; $^{\$}P < 0.05$ versus values at 1.0 Hz; $^{\clubsuit}P < 0.05$ versus values in LVMMs at 1.0 Hz; $^{\clubsuit}P < 0.05$ versus values in LVMMs at 0.5 Hz.
APD, action potential duration; APD_{50} and APD_{90}, duration of the AP at 50 and 90% repolarization; EADs, early afterdepolarizations; LVMMs, left ventricular midmyocardial myocytes; PFs, Purkinje fibres; STV, short-term variability.

more, during the transition to the steady-state decrease in APD in LVMMs (Figure 2B), terfenadine induced a marked increase in temporal BVR at 1 Hz. Figure 2A shows that prior to the shortening effect of 1 μM terfenadine, the progression to the plateau phase of the AP, but not APD, was affected (traces 1, 100 and 150). Although between traces 170 and 198, the right shift of the progression phase became more pronounced, and the plateau phase was depressed, APD was not affected, and terfenadine caused the loss of AP dome. During the transition to the steady-state decrease in APD (traces 198 to 227; Figure 2B), large variations in successive APDs were seen (Figure 2A). This shortening-effect generated large complex polygons ascribing the differences in APDs with numerous points lying distant from the identity line of the Poincaré plot (Figure 2C). Four out of 10 myocytes showed this increase in temporal BVR that returned towards vehicle values at 10 μM. Finally, of the six cells not showing this change at 1 μM, two were not tested at 10 μM, and two of the remaining four cells showed the same response. Relative to the vehicle values in these six myocytes showing an increase in BVR, terfenadine increased STV(APD_{90}) during the transition to the steady-state decrease in APD, and this increase in STV(APD_{90}) returned towards vehicle values at steady state (Figure 2D). Similar findings were seen for STV(APD_{50}) (Figure 2A, average data not shown). While in PFs, a significant increase in triangulation was seen at 10 μM during 1 Hz, terfenadine in LVMMs evoked a triangular pattern of steady-state decrease in APD that became statistically significant at 1 and 10 μM during 1 and 0.5 Hz respectively (Table 3). However, triangulation was not increased in the six myocytes showing an increase in temporal BVR (1.17 ± 0.03 during the transition from a vehicle value of 1.14 ± 0.02, $P > 0.05$ *vs.* vehicle).

Pinacidil and diltiazem. No significant change in STV(APD_{90}) was observed in PFs at either 1 Hz or 0.5 Hz pacing frequency after exposure to pinacidil (Table 4). In LVMMs – whereas over the concentration range 0.01–10 μM, STV(APD_{90}) was not significantly changed – pinacidil (30 μM) decreased the fluctuation of consecutive APs, and this was reflected by a marked decrease in STV(APD90) at 1 and 0.5 Hz (Table 4). Similar findings were observed for STV(APD_{50}) (data not shown). Additionally, pinacidil caused a concentration-dependent increase in triangulation at 1 Hz in both preparations, and the increase in triangulation tended not to be different during low pacing frequency (Table 4).

Over the concentration range tested, no significant change in STV(APD_{90}) was observed in PFs at either 1 or 0.5 Hz pacing frequency after exposure to diltiazem (Table 4). Although similar data were obtained in LVMMs (Table 4), diltiazem (30 μM) induced a marked increase in temporal BVR at 1 Hz during the transition to the steady-state decrease in APD in one experiment only (data from this cell were not included in the average data shown in Table 4). Similar findings were

Table 4 Effects of pinacidil and diltiazem on STV(APD_{90}) and triangulation (ratio of APD_{90}/APD_{50}) as a function of change in APD_{90} in dog PFs and LVMMs

Drug	*Preparation*	*Animals*	*n*	*Pacing*	*Parameter*	*Baseline*	*Nominal concentrations tested*					
Pinacidil							0.01 μM	0.1 μM	1 μM	3 μM	10 μM	30 μM
	PF	4	4	1.0 Hz	APD_{90} (ms)	291 ± 16	0.3 ± 2%	−1 ± 3%	−18 ± 5%*	−42 ± 6%#♣		
					STV(APD_{90}) (ms)	0.4 ± 0.1♣	0.6 ± 0.2♣	0.4 ± 0.1♣	0.4 ± 0.1♣	0.4 ± 0.1♣		
					Triangulation	1.60 ± 0.18	1.61 ± 0.18	1.59 ± 0.49	1.95 ± 0.39♣	2.84 ± 0.67*♣		
				0.5 Hz	APD_{90} (ms)	331 ± 27	1 ± 2%	−1 ± 4%	−21 ± 7%*	−47 ± 8%#♣		
					STV(APD_{90}) (ms)	0.7 ± 0.3♣	0.5 ± 0.1♣	0.4 ± 0.1♣	0.6 ± 0.3♣	0.6 ± 0.3♣		
					Triangulation	1.68 ± 0.22	1.78 ± 0.23	1.68 ± 0.24	2.10 ± 0.48♣	3.16 ± 0.88*♣		
	LVMM	3–7	1	1.0 Hz	APD_{90} (ms)	397 ± 18	−2 ± 0.2%	0.2 ± 1%	−8 ± 2%#	−9 ± 2%*	−51 ± 3%#	−86 ± 1%#
					STV(APD_{90}) (ms)	10 ± 1	8 ± 1	8 ± 1	9 ± 1	8 ± 1	10 ± 1	2 ± 0.2#
					Triangulation	1.18 ± 0.03	1.13 ± 0.01	1.13 ± 0.01	1.19 ± 0.03	1.14 ± 0.01	1.45 ± 0.07*	2.57 ± 0.25*
				0.5 Hz	APD_{90} (ms)	457 ± 37	0.6 ± 0.8%	2 ± 1%	−10 ± 2%#	−4 ± 2%	−47 ± 6%#	−86 ± 2%#
					STV(APD_{90}) (ms)	22 ± 8	13 ± 1	12 ± 3	13 ± 2	9 ± 1	8 ± 1	2 ± 0.4*
					Triangulation	1.17 ± 0.03	1.12 ± 0.01	1.12 ± 0.01	1.18 ± 0.03	1.13 ± 0.01	1.39 ± 0.04#	2.59 ± 0.29*
Diltiazem							1 μM	3 μM	10 μM	30 μM		
	PF	5	5	1.0 Hz	APD_{90} (ms)	321 ± 19	−2 ± 0.2%	−3 ± 1%	−4 ± 2%♣	−12 ± 4%*♣		
					STV(APD_{90}) (ms)	0.6 ± 0.2♣	0.7 ± 0.3♣	1.2 ± 0.4♣	1.1 ± 0.5♣	0.9 ± 0.2♣		
					Triangulation	1.25 ± 0.02♣	1.30 ± 0.03♣	1.39 ± 0.03#♣	1.86 ± 0.05#♣	3.18 ± 0.23#♣		
				0.5 Hz	APD_{90} (ms)	362 ± 26	−0.5 ± 1%	0 ± 2%	−1 ± 2%	−10 ± 4%*♣		
					STV(APD_{90}) (ms)	0.9 ± 0.3♣	1.3 ± 0.4♣	1.1 ± 0.3♣	2.2 ± 1.1	1.0 ± 0.3♣		
					Triangulation	1.26 ± 0.02♣	1.29 ± 0.03♣	1.39 ± 0.02#♣	1.84 ± 0.05#♣	3.18 ± 0.14#♣		
	LVMM	4–5	2	1.0 Hz	APD_{90} (ms)	368 ± 30	−4 ± 1%	−4 ± 5%	−25 ± 6%*	−41 ± 4%#		
					STV(APD_{90}) (ms)	5 ± 1	5 ± 1	5 ± 1	7 ± 2	6 ± 1		
					Triangulation	1.18 ± 0.02	1.18 ± 0.01	1.18 ± 0.02	1.24 ± 0.03	1.37 ± 0.08*		
				0.5 Hz	APD_{90} (ms)	422 ± 41	−7 ± 1%	−2 ± 1%	−18 ± 6%*	−34 ± 5%#		
					STV(APD_{90}) (ms)	6 ± 1	7 ± 3	5 ± 1	4 ± 1	4 ± 1*		
					Triangulation	1.17 ± 0.01	1.16 ± 0.01	1.16 ± 0.02	1.20 ± 0.02	1.36 ± 0.09*		

Changes in APD_{90}, STV(APD_{90}) and triangulation were measured once steady state was achieved.
*$P < 0.05$ and #$P < 0.01$ versus values from vehicle; $P < 0.05$ versus values at 1.0 Hz; ♣$P < 0.05$ versus values in LVMMs at 1.0 Hz; ♠$P < 0.05$ versus values in LVMMs at 0.5 Hz.
APD, action potential duration; APD_{50} and APD_{90}, duration of the AP at 50 and 90% repolarization; LVMMs, left ventricular midmyocardial myocytes; PFs, Purkinje fibres; STV, short-term variability.

Table 5 Effects of reference drugs on APD_{50} in dog PFs and LVMMs

Drug	*APD*	*Preparation*	*Pacing*	*Baseline*	*Nominal concentrations tested*					
Dofetilide					0.001 μM	0.01 μM	0.1 μM	1 μM		
	APD_{50} (ms)	PF	1.0 Hz	213 ± 8	12 ± 5%*	44 ± 4%#♣	75 ± 8%#	94 ± 6%#♣		
			0.5 Hz	240 ± 11	11 ± 6%	54 ± 5%#♠	101 ± 9%#$♠	131 ± 10%#$		
		LVMM	1.0 Hz	316 ± 16	1 ± 1%	12 ± 4%*	36 ± 13%#	46 ± 14%*		
			0.5 Hz	377 ± 15	−2 ± 1%	14 ± 4%*	40 ± 15%*	62 ± 13%*		
d-sotalol					1 μM	10 μM	30 μM	100 μM		
	APD_{50} (ms)	PF	1.0 Hz	188 ± 11	1 ± 3%	16 ± 4%*	35 ± 9%*	53 ± 11%*		
			0.5 Hz	207 ± 13	2 ± 1%	18 ± 5%*	43 ± 11%*	67 ± 18%*		
		LVMM	1.0 Hz	303 ± 14	−3 ± 1%	11 ± 3%*	14 ± 4%*	27 ± 5%#		
			0.5 Hz	341 ± 16	−4 ± 4%	9 ± 10%	30 ± 17%*	49 ± 11%*		
dl-sotalol					1 μM	10 μM	30 μM	100 μM		
	APD_{50} (ms)	LVMM	1.0 Hz	272 ± 17	−0.5 ± 1%	8 ± 2%#	10 ± 3%*	19 ± 4%#		
			0.5 Hz	315 ± 21	−3 ± 1%	3 ± 2%	9 ± 3%*	24 ± 7%#		
Cisapride					0.01 μM	0.1 μM	1 μM	10 μM		
	APD_{50} (ms)	PF	1.0 Hz	266 ± 18	5 ± 3%	12 ± 3%#♣	8 ± 9%	−36 ± 6%#		
			0.5 Hz	294 ± 22	5 ± 5%	16 ± 6%*♠	31 ± 11%*	−22 ± 8%*		
		LVMM	1.0 Hz	300 ± 17	3 ± 3%	32 ± 10%#	15 ± 5%*	−22 ± 7%*		
			0.5 Hz	332 ± 19	8 ± 2%	49 ± 7%#	37 ± 3%#$	−24 ± 11%*		
Terfenadine					0.01 μM	0.1 μM	1 μM	10 μM		
	APD_{50} (ms)	PF	1.0 Hz	218 ± 14	3 ± 2%	1 ± 0.9%	2 ± 3%♣	−11 ± 4%*♣		
			0.5 Hz	237 ± 22	2 ± 1%	2 ± 0.8%	3 ± 2%♠	−5 ± 2%♠		
		LVMM	1.0 Hz	320 ± 14	−1 ± 1%	4 ± 1%*	−40 ± 6%#	−78 ± 2%#		
			0.5 Hz	369 ± 20	−0.4 ± 1%	6 ± 2%*	−20 ± 6%#$	−72 ± 3%#		
Pinacidil					0.01 μM	0.1 μM	1 μM	3 μM	10 μM	30 μM
	APD_{50} (ms)	PF	1.0 Hz	190 ± 19	0 ± 2%	0 ± 3%	−28 ± 8%*	−64 ± 5%#		
			0.5 Hz	205 ± 20	−4 ± 6%	−1 ± 5%	−31 ± 10%*	−67 ± 7%#♠		
		LVMM	1.0 Hz	333 ± 8	−1 ± 0.3%	−0.5 ± 1%	−8 ± 2%#	−9 ± 1%*♣	−58 ± 5%#	−93 ± 1%#
			0.5 Hz	386 ± 19	1 ± 1%	2 ± 1%	−11 ± 2%#	−4 ± 2%	−54 ± 5%#	−92 ± 1%#
Diltiazem					1 μM	3 μM	10 μM	30 μM		
	APD_{50} (ms)	PF	1.0 Hz	257 ± 18	−5 ± 0.7%	−13 ± 1%#	−35 ± 3%#	−64 ± 3%#		
			0.5 Hz	289 ± 24	−3 ± 0.9%	−9 ± 1%#♠	−32 ± 3%#	−64 ± 3%#		
		LVMM	1.0 Hz	309 ± 23	−4 ± 2%	−4 ± 6%	−28 ± 7%*	−48 ± 6%#		
			0.5 Hz	352 ± 30	−6 ± 2%	−0.2 ± 2%	−19 ± 7%*	−41 ± 8%#		

*$P < 0.05$ and #$P < 0.01$ versus values from vehicle; $$P < 0.05$ versus values at 1.0 Hz; ♣$P < 0.05$ versus values in LVMMs at 1.0 Hz; ♠$P < 0.05$ versus values in LVMMs at 0.5 Hz.
APD, action potential duration; APD_{50} and APD_{90}, duration of the AP at 50 and 90% repolarization; LVMMs, left ventricular midmyocardial myocytes; PFs, Purkinje fibres; STV, short-term variability.

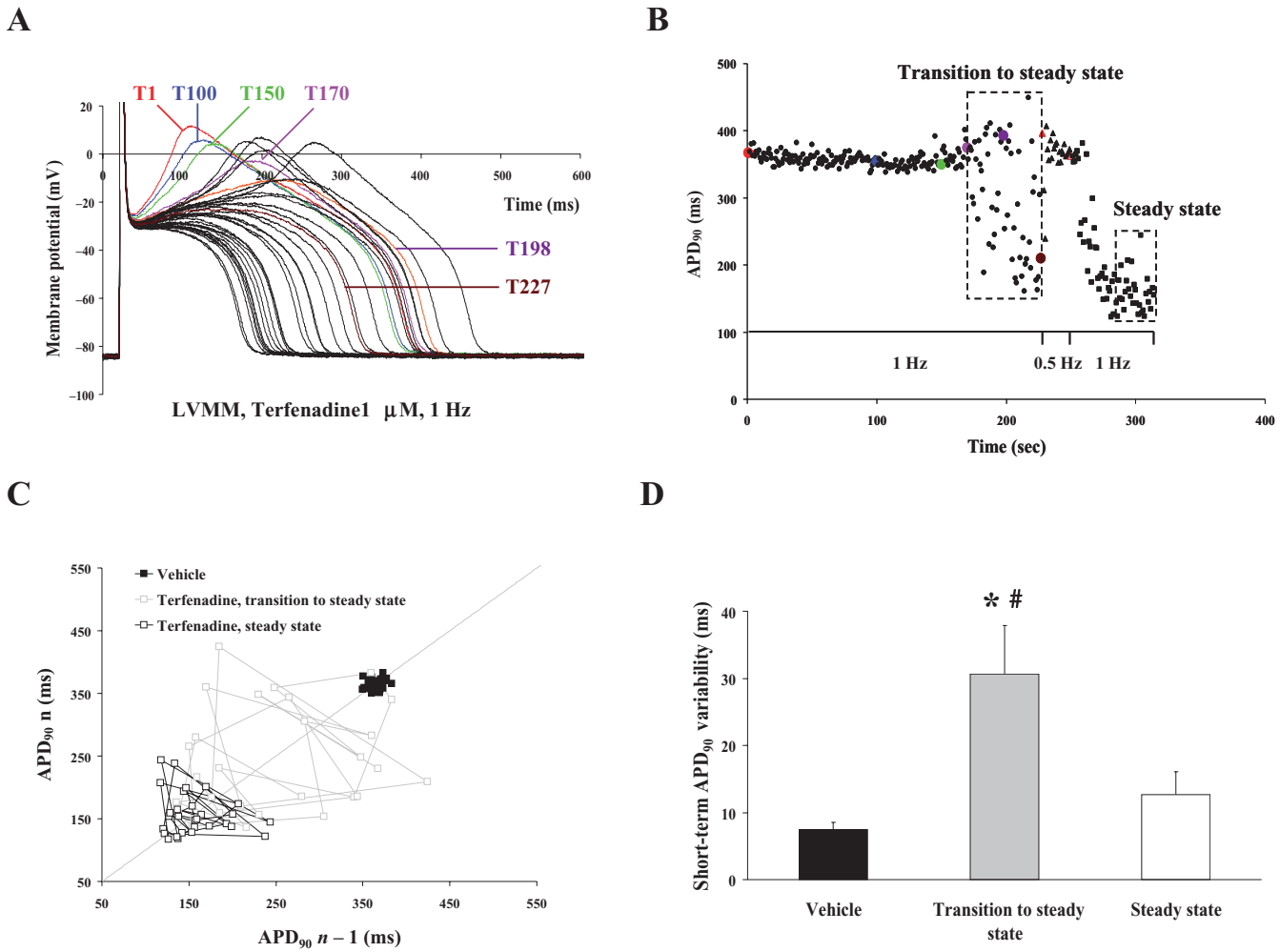

Figure 2 Effect of terfenadine on STV(APD) during the transition to the steady-state decrease in APD. (A) Typical large variations in successive APDs (black traces 198 to 227) were seen in a left ventricular midmyocardial myocyte (LVMM), after exposure to terfenadine (1 μM), at pacing frequency of 1 Hz. This is an example of temporal dispersion of repolarization within a single cell during the transition to the steady-state decrease in APD. (B) Shows the time course of the same cell as in Figure 2A during the perfusion of terfenadine (1 μM) (dashed rectangles illustrate the periods of transition to steady state and steady state; red filled and unfilled triangles illustrate the changes from 1 to 0.5 Hz and back to 1 Hz, respectively; coloured filled circles illustrate the time at which coloured AP traces of Figure 2A were selected). (C) Shows a representative example of a Poincaré plot of APD_{90} from a LVMM (same cell as in A) under vehicle (0.1% DMSO) and in the presence of 1 μM terfenadine (during transition to steady state and at steady state). Note the large complex polygons during the transition to the steady-state decrease in APD. (D) Increasing STV(APD_{90}) during the transition to the steady-state decrease in APD_{90} [$n = 6$ cells (two dogs)]. $^{*}P < 0.05$ versus vehicle and $^{\#}P < 0.05$ *versus* steady state. APD, action potential duration; DMSO, dimethylsulphoxide; LVMM, left ventricular midmyocardial myocyte; STV, short-term variability.

observed for STV(APD_{50}) (data not shown). Finally, triangulation in both preparations was increased when AP was shortened by diltiazem during 1 Hz, and the increase in triangulation was not different during 0.5 Hz (Table 4). Moreover, the increase in triangulation was lower in LVMMs compared with PFs, and this was due to the fact that the decreasing-effects of diltiazem on APD_{50} and APD_{90} were similar in LVMMs (Tables 4 and 5).

Relation between EAD incidence and changes in APD, STV(APD) or triangulation in LVMMs

Thomsen *et al.* (2004) showed that proarrhythmia is not related to differences in prolongation of repolarization, but corresponds to BVR in midmyocardial myocytes isolated from dogs with chronic AV block (CAVB). Therefore, data from a total of 11 LVMMs isolated from dogs with normal sinus rhythm were examined to determine the relation between EAD incidence and changes in APD, STV(APD) or triangulation during maximal I_{Kr} block with 1 μM dofetilide. In the cells treated with 1 μM dofetilide, 6 of 11 showed EADs, which divided the population. STV(APD_{90}), but not triangulation, at baseline were different in these two groups at a pacing frequency of either 1 (Figure 3E) or 0.5 Hz (Figure 3F). Although APD_{90} increase after exposure to dofetilide was similar in the two groups at 1 Hz, STV(APD_{90}), but not triangulation, increased and was significantly larger in the group with EADs (Figure 3E). Despite this increase in STV(APD_{90}) in the group with EADs, no incidence of EADs was seen at this pacing frequency (Figure 3C). Moreover, although dofetilide-

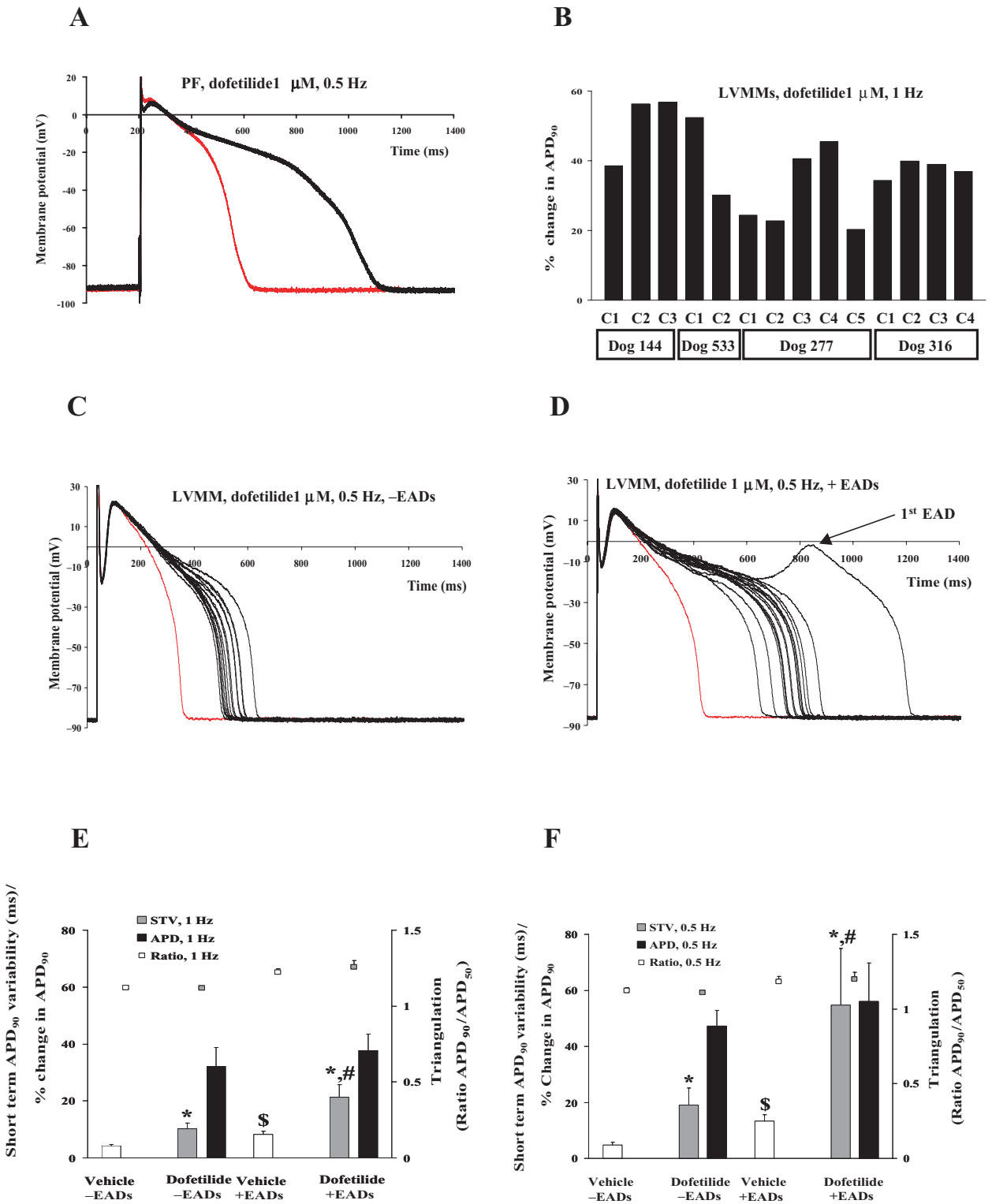

Figure 3 (A) Fifteen consecutive APs recorded from a PF at a pacing frequency of 0.5 Hz before (red line) and under the influence of 1 μM dofetilide. Note the absence of temporal dispersion of APD. (B) APD_{90} increases at 1 Hz pacing frequency after exposure to dofetilide (1 μM) in 14 LVMM cells (four dogs). Note the effects on APD_{90} are largely independent of isolations in LVMMs. (C and D) Fifteen consecutive APs recorded from two LVMMs representing cells with (D) and without (C) EADs. Pacing frequency is 0.5 Hz before (red line) and under the influence of 1 μM dofetilide. Note the presence of temporal dispersion of APD. (E and F) Composite data grouped according to presence of EADs at I_{Kr} block. STV(APD_{90}) (open bars) and triangulation (open squares) were measured at baseline and during block of I_{Kr} before first EAD (right) or once steady state was achieved (left) during a pacing frequency of either 1 Hz (E) or 0.5 Hz (F). Note the change in APD_{90} under the influence of 1 μM dofetilide (black bars). n = 11 cells (three dogs). *P < 0.05 versus vehicle, $^{\$}P$ < 0.01 versus vehicle (– EADs) and $^{\#}P$ < 0.05 dofetilide (– EADs). AP, action potential; APD, action potential duration; APD_{50} and APD_{90}, duration of the AP at 50% and 90% repolarization; EADs, early afterdepolarizations; LVMMs, left ventricular midmyocardial myocytes; STV, short-term variability.

induced increases in APD_{90} and $STV(APD_{90})$ in both groups were greater at 0.5 Hz compared with 1 Hz pacing frequency, APD_{90} increase after exposure to dofetilide was similar in the two groups, and $STV(APD_{90})$ was significantly greater in the group with EADs (Figure 3F), and the increased $STV(APD_{90})$ clearly preceded the occurrence of the first EAD (Figure 3D). Additionally, no triangular pattern of APD prolongation was evoked by dofetilide at 0.5 Hz (Figure 3F). Hence, these data expose the eventual proarrhythmic potential of reduced pacing frequency, and that the higher the STV is during low pacing frequency, the greater the likelihood for EADs.

Discussion

The main findings of the present study were as follows: (i) beagle dog LVMMs provided stable recordings of AP and can be used to screen out unwanted drug effects on APD in safety pharmacology studies; (ii) these normal, unremodelled, mid-myocardial myocytes responded with a proarrhythmic response to I_{Kr} blockers; and (iii) EAD incidence was not related to differences in APD prolongation or triangulation but did correspond to BVR, here quantified as STV of APD.

LVMMs as a preclinical model for the assessment of drug-induced changes in APD

In contrast to recent data obtained from guinea pig ventricular myocytes (Zaniboni *et al.*, 2000; Terrar *et al.*, 2007), AP parameters in beagle LVMMs were found to be very stable (Figure 1A and B). Furthermore, sequential vehicle additions did not significantly affect APD (Figure 1E and F), thus illustrating they can be used to generate four-point concentration-effect curves. Additionally, because neither STV(APD) nor triangulation changes were seen over time (Figure 1C and D) or during the sequential additions of vehicle (Figure 1E and F), beagle LVMMs can be used to measure putative indices of proarrhythmic risk.

The effects of reference drugs on the AP in canine PFs have already been reported (Gintant *et al.*, 2001; Lu *et al.*, 2001; 2007; Abi-Gerges *et al.*, 2004; Champeroux *et al.*, 2005; Terrar *et al.*, 2007). These effects were confirmed in the present study (Tables 2–5). Additionally, responses to these drugs in LVMMs are comparable with PFs, with the exception of terfenadine (Tables 2–5). Although a potent inhibitor of I_{Kr} (Crumb, 2000), significant prolongation of APD with terfenadine was observed in LVMMs, and this was a relatively small prolongation at 10 times the maximum effective free therapeutic plasma concentration ($EFTPC_{max}$) (QT prolongation in humans is observed at this multiple of $EFTPC_{max}$; Pratt *et al.*, 1996) that was reversed at higher concentrations (111 times the $EFTPC_{max}$; Tables 1, 3 and 5). In agreement with recent studies that used dog and rabbit preparations (Gintant *et al.*, 2001; Masumiya *et al.*, 2004; Terrar *et al.*, 2007), this study confirms that terfenadine did not significantly affect APD in PFs, except for a small decrease in APD_{50} seen at 10 μM (Tables 3 and 5), an effect that may relate to its inhibitory effect on I_{Ca} (inward cardiac Ca^{2+} current) (Ming and Nordin, 1995; Li *et al.*, 2006). Moreover, while the maximum prolongation of APD achieved in guinea pig myocytes (Davie *et al.*, 2004; Terrar *et al.*, 2007) and beagle LVMMs (Tables 3 and 5) was seen in the presence of terfenadine at 10 times $EFTPC_{max}$, a lower concentration was needed to shorten the AP in beagle LVMMs (Tables 3 and 5) compared with guinea pig (Terrar *et al.*, 2007). Therefore, it can be postulated that the potency of terfenadine for I_{Ca} would be greater in beagle LVMMs compared with guinea pig ventricular myocytes. Thus, the data presented in this study suggest that (i) beagle LVMMs show good sensitivity for detecting APD prolongation with multiple ion channel inhibitors like terfenadine and cisapride, most notably at concentrations closest to their IC_{50} (molar concentration of a drug producing 50% inhibition) values on I_{Kr} (Redfern *et al.*, 2003); and (ii) effects of terfenadine may vary in *in vitro* AP assays using tissues from the same species.

Compared with PFs, the throughput with LVMMs is fourfold higher, animal demand is reduced fourfold, and there is no diffusion barrier to limit drug access. Additionally, since repolarization of the VMMs usually determines the end of the T-wave (Antzelevitch, 2007), data from these myocytes may correlate better with QT measurements in dogs and humans. This latter assumption is based on the observation that the distribution of ion channel proteins and ionic currents that determine the AP shape and duration are similar in dog and human ventricles (Szabo *et al.*, 2005). Therefore, LVMMs can be used as a preclinical model for the assessment of drug-induced changes in APD at a late phase of the drug discovery process. Moreover, because of significant regulatory pressure to ensure that there is no QT prolongation in the corresponding clinical study (Anon, 2005b), significant effort has been devoted to developing preclinical strategies to minimize and detect QT prolongation risk at a relatively early phase of drug discovery (Pollard *et al.*, 2008). This would be ideally achieved by measuring the AP in native myocytes (i.e. an integrated system). However, because the volume of testing required prevents this, pharmaceutical companies have sought to molecularise the AP. However, no matter how comprehensive the panel of molecular targets may be, it cannot reproduce an integrated system. Thus, development and usage of a high-throughput LVMM assay for effects on AP to be used at an early phase of drug discovery may help to develop potential drugs with no QT prolongation risk and reduce cardiac safety-related attrition of new drug candidates.

Temporal STV(APD) may predict the proarrhythmic potential of a drug

STV of repolarization, but not QT prolongation, is thought to be a good predictor of a torsadogenic risk (Milberg *et al.*, 2004; Thomsen *et al.*, 2004; 2006; Lengyel *et al.*, 2007; So *et al.*, 2008). The results of the present study support this finding and confirm that EAD incidence in LVMMs after exposure to I_{Kr} blockers is not related to differences in APD prolongation or triangulation, but corresponds to the STV(APD) that preceded EADs (Figure 3). Additionally, our data show the eventual proarrhythmic potential of reduced pacing frequency and that the higher the STV during low pacing frequency, the greater the likelihood of EADs (Figure 3E and F). In contrast, I_{Kr} blockers failed to increase STV(APD) in other studies

(Michael *et al.*, 2007; 2008; Thomsen *et al.*, 2007). Although investigators studied the proarrhythmic potential and EAD incidence under conditions of attenuated repolarization due to drugs (Volders *et al.*, 2003; Lengyel *et al.*, 2007; Guérard *et al.*, 2008; So *et al.*, 2008) or remodelling (Volders *et al.*, 1998; Thomsen *et al.*, 2004; 2006), our data are the first to show that selective I_{Kr} blockers as a single cause can induce EADs in normal, unremodelled, LVMMs. This finding is not consistent with data reported by Biliczki *et al.* (2002), who investigated the effects of dofetilide in dog right ventricular papillary muscle. A likely explanation for these opposing results is the different repolarizing behaviour of LVMMs versus papillary muscle of the right ventricle. Moreover, although d- and dl-sotalol prolonged the AP in LVMMs, only d-sotalol increased STV(APD) (Tables 2 and 5), and, consequently, EAD episodes were observed. Thus, the preparation of beagle LVMMs predicted the proarrhythmic potential of d-sotalol and the antiarrhythmic property of dl-sotalol. As d-, l- and dl-sotalol were shown to have the same potency at I_{Kr} (Carmeliet, 1985; N Abi-Gerges J-P Valentin and Chris E Pollard unpubl. data), this suggests that the I_{Kr} blocking effect of dl-sotalol is not reduced compared with d-sotalol. These effects on I_{Kr} current are in agreement with studies that reported a lengthening of the AP and the effective refractory period by d-, l- and racemic (dl-) sotalol (Carmeliet, 1985; Lathrop, 1985; Kato *et al.*, 1986; Manley *et al.*, 1986; Tande and Refsum, 1988). Additionally, d-sotalol was one- to three-fold more potent than either l-sotalol or the racemate in inducing AP prolongation (Lathrop, 1985). Other studies demonstrated a weak β-adrenoceptor-blocking activity of d-sotalol compared with l-sotalol (Gomoll and Bartek, 1986; Manley *et al.*, 1986; Tande and Refsum, 1988). Taken together, all these data suggest that the blockade of the β-adrenoceptors by the l-element in dl-sotalol may play a role in the divergent results of d- and dl-sotalol on STV(APD). Moreover, our findings with dl-sotalol are not consistent with those reported in the rabbit Langendorff heart model (Lawrence *et al.*, 2006). Overall, explanations for these divergent STV(APD) results with these I_{Kr} blockers are likely to involve species differences and/or the different areas of the left ventricle (epicardium, midmyocardium and endocardium), which may exhibit different sensitivities to changes in repolarization. Furthermore, the absence of triangulation after exposure to dofetilide and d-sotalol in LVMMs is consistent with data reported in dog CAVB (Thomsen *et al.*, 2004), guinea pig myocytes (Davie *et al.*, 2004) and an open-chest, pentobarbital-anaesthetized, α_1-adrenoceptor-stimulated rabbit model after treatment with E-4031 (Michael *et al.*, 2007). On the other hand, our data do not accord with the triangulation findings of recent investigations in beagle PFs (Champeroux *et al.*, 2005), rabbit Langendorff heart model (Milberg *et al.*, 2004; Lawrence *et al.*, 2006) and guinea pig myocytes (Terrar *et al.*, 2007).

As observed with dofetilide and d-sotalol, cisapride increased STV(APD) in LVMMs, and temporal BVR preceded EADs, although its effect on STV(APD) was biphasic (Table 3). This biphasic action of cisapride on STV(APD) correlates well with its effects on APD (Table 3). While the increase in STV(APD) and occurrence of EADs in the absence of triangulation can be associated with I_{Kr} inhibition (Mohammad *et al.*, 1997), inhibition of I_{Na} and/or I_{Ca} currents increased triangulation, reversed the increase in STV(APD) (Table 3), and, consequently, EADs were not observed. Although these three drugs had no effects on STV(APD), frequency-dependent APD prolongation and cisapride-induced increase in triangulation (Tables 2 and 3) did not lead to EAD incidence in PFs. Thus, APD prolongation, reduced frequency and triangulation are not good predictors of arrhythmogenic potential in PF preparations. However, EAD incidence was seen at 0.2 Hz in PFs of rabbit (sparfloxacin-enhanced BVR, Lu *et al.*, 2006) and beagle (Abi-Gerges *et al.*, 2004) hearts and guinea pig ventricular myocytes (Davie *et al.*, 2004). Altogether, these data suggest that pacing frequency may differentially influence temporal BVR in tissues from the same source (this study) and between species (dog vs. guinea pig myocytes). Finally, our results in LVMMs support the findings of some earlier investigators, who proposed that susceptibility to proarrhythmia is related not only to spatial, but also to temporal, BVR (Berger *et al.*, 1997; Hondeghem *et al.*, 2001).

Despite being a multi-channel blocker, terfenadine showed a distinctive proarrhythmic potential profile (Figure 2, Table 3) compared with cisparide. Changes seen in the AP plateau phase (Figure 2A) suggest a possible role for I_{Ca} in the marked increase in STV(APD) evoked by terfenadine during the transition to the steady-state decrease in APD (Figure 2B). This is consistent with previously reported findings that terfenadine reduced I_{Ca} significantly (Ming and Nordin, 1995; Li *et al.*, 2006). The present investigation is the first to report an increase in temporal STV(APD) in myocytes after exposure to terfenadine. Given that triangulation was not increased during the transition to a steady-state decrease in APD and QT prolongation in humans (Pratt *et al.*, 1996), APD increase (this study) was seen at 10 times $EFTPC_{max}$, increased temporal BVR during the transition phase at 111 times $EFTPC_{max}$ may play a role in terfenadine-induced TdP in humans. Our BVR data with terfenadine are consistent with those reported in the rabbit Langendorff heart model (Hondeghem *et al.*, 2001). In that study, the worst proarrhythmia was observed when increased temporal instability coincided with shortening of the AP. In addition, amiodarone (another multi-channel blocker) elicited instability and triangulation, but caused no proarrhythmia (Hondeghem and Hoffmann, 2003). This abnormal behaviour may result from the fact that amiodarone blocks inward currents, and block of these currents has been shown to attenuate or reverse class III proarrhythmia (Carlsson *et al.*, 1993; Hohnloser *et al.*, 1994). When taken together, the data from terfenadine and amiodarone suggest that blockade of inward currents by multi-channel blockers may not always protect against proarrhythmia. Additionally, STV(APD) behaviour like that of terfenadine was seen to a lesser extent (1 out of 6 cells) during exposure to ditiazem (an I_{Ca} antagonist) and not at all with pinacidil (an I_{KATP} opener). Additionally, triangulation seen with pinacidil and diltiazem is unlikely to increase the risk of repolarization arrhythmias without an increase in STV(APD) (Table 4). Our triangulation data with diltiazem are consistent with those reported in beagle and rabbit PFs (Champeroux *et al.*, 2005; Lu *et al.*, 2007) and in guinea pig ventricular myocytes with two other I_{Ca} antagonists (nifedipine and verapamil) (Terrar *et al.*, 2007), although they are not consistent with those reported by Lawrence *et al.* (2006).

Finally, it is important that further investigations are carried out to evaluate how triangulation might be related to an increased risk of proarrhythmia. A recent study in rabbit ventricular myocytes indicates that AP triangulation accelerated I_{Ca} recovery from inactivation, which increases the risk of inducing EADs (Guo *et al*., 2007).

It is suggested that cell-to-cell coupling would attenuate temporal BVR in multicellular preparations compared with isolated myocytes (Poelzing and Rosenbaum, 2004; Spitzer *et al*., 2006). This is confirmed in this study under baseline conditions (Figure 1E and F; Tables 2, 3 and 4). Thus, drug effects on AP fluctuations may have been enhanced by the lack of electrotonic interactions in LVMMs. Based on MAPD and QT data, however, it could be concluded that STV was found to increase and decrease along with the proarrhythmic risk in Langendorff-perfused rabbit (Hondeghem and Hoffmann, 2003; Hondeghem *et al*., 2003; Lawrence *et al*., 2006) and intact dog (Thomsen *et al*., 2006; 2007; Gallacher *et al*., 2007) hearts. Moreover, the action of cisapride on STV(APD) in LVMMs (Table 3) shows an STV behaviour that heralds impending EAD incidence when proarrhythmic conditions are applied and *vice versa*. Furthermore, an enhancer of cell-to-cell coupling reduced, but did not entirely suppress, EAD genesis and TdP incidence evoked by anemone toxin II in an arterially perfused ventricular wedge preparation of rabbit hearts (Quan *et al*., 2007). Altogether, these data suggest that electrotonic coupling does not completely dampen proarrhythmic STV behaviour, although it may decrease such activity. Further studies are necessary to determine the influence of cell-to-cell coupling on BVR.

In summary, the results of the present investigation suggest that beagle dog LVMMs not only provide a suitable preclinical model to assess unwanted drug effects on APD, but also yield additional information about putative indicators of proarrhythmia that can add value to an integrated QT/TdP risk assessment. Our findings further emphasize that increased temporal BVR [quantified as STV(APD)] may predict drug-induced proarrhythmia.

Acknowledgements

The authors express their gratitude to Jackie A. Moors, Sue Egerton, Ann J. Woods, Sally Luke, Ben G Small, Dr Karen L Philp, Dr Chris L Lawrence and Dr Philip Jarvis for their expert technical assistance, and wish to thank Jordi Heijman for developing the AP Analytical Tool. The authors would also like to thank Dr Leif G Carlsson for critical review of the manuscript.

Conflict of interest

The authors state no conflict of interest.

References

Abi-Gerges N, Small BG, Lawrence CL, Hammond TG, Valentin JP, Pollard CE (2004). Evidence for gender differences in electrophysiological properties of canine Purkinje fibres. *Br J Pharmacol* **142**: 1255–1264.

Anon (2000). *Committee for Proprietary Medicinal Products (CPMP). Safety pharmacology studies for human pharmaceuticals. The European Agency for the evaluation of medicinal products*. London, November 16, 2000. Reference CPMP/ICH/539/00.

Anon (2005a). *ICH S7B Note for guidance on the nonclinical evaluation of the potential for delayed ventricular repolarization (QT interval prolongation) by human pharmaceuticals*. London, 25 May. Reference CHMP/ICH/423/02.

Anon (2005b). *ICH E14 Note for guidance on the clinical evaluation of QT/QTc interval prolongation and proarrhythmic potential for non-antiarrhythmic drugs*. London, 25 May. Reference CHMP/ICH/2/04.

Antzelevitch C (2007). Heterogeneity and cardiac arrhythmias: an overview. *Heart Rhythm* **4**: 964–972.

Balati B, Varro A, Papp JG (1998). Comparison of the cellular electrophysiological characteristics of canine left ventricular epicardium, M cells, endocardium and Purkinje fibres. *Acta Physiol Scand* **164**: 181–190.

Bass A, Valentin J-P, Fossa AA, Volders PG (2007). Points to consider emerging from a mini-workshop on cardiac safety: assessing torsades de pointes liability. *J Pharmacol Toxicol Methods* **56**: 91–94.

Berger RD, Kasper EK, Baughman KL, Marban E, Calkins H, Tomaselli GF (1997). Beat-to-beat QT interval variability: novel evidence for repolarization lability in ischemic and nonischemic dilated cardiomyopathy. *Circulation* **96**: 1557–1565.

Biliczki P, Virág L, Iost N, Papp JG, Varró A (2002). Interaction of different potassium channels in acrdiac repolarization in dog ventricular preparations: role of repolarization reserve. *Br J Pharmacol* **137**: 361–368.

Carlsson L, Drews L, Duker G, Schiller-Linhardt G (1993). Attenuation of proarrhythmias related to delayed repolarization by low-dose lidocaine in the anesthetized rabbit. *J Pharmacol Exp Ther* **267**: 1076–1080.

Carmeliet E (1985). Electrophysiologic and voltage clamp analysis of the effects of sotalol on isolated cardiac muscle and Purkinje fibers. *J Pharmacol Exp Ther* **232**: 817–825.

Cavero I, Mestre M, Guillon JM, Heuillet E, Roach AG (1999). Preclinical in vitro cardiac electrophysiology: a method of predicting arrhythmogenic potential of antihistamines in humans? *Drug Safety* **21** (Suppl. 1): 19–31.

Champeroux P, Viaud K, El Amrani AI, Fowler JS, Martel E, Le Guennec JY *et al*. (2005) Prediction of the risk of torsade de pointes using the model of isolated canine Purkinje fibres. *Br J Pharmacol* **144**: 376–385.

Crumb WJ Jr (2000). Loratadine blockade of K+ channels in human heart: comparison with terfenadine under physiological conditions. *J Pharmacol Exp Ther* **292**: 261–264.

Davie C, Valentin J-P, Pollard C, Standen N, Mitcheson J, Alexander P *et al*. (2004). Comparative pharmacology of guinea pig cardiac myocyte and cloned hERG (IKr) channel. *J Cardiovasc Electrophysiol* **15**: 1302–1309.

Fenichel RR, Malik M, Antzelevitch C, Sanguinetti M, Roden DM, Priori SG *et al*. (2004). Drug-induced torsades de pointes and implications for drug development. *J Cardiovasc Electrophysiol* **15**: 475–495.

Gallacher DJ, Van de Water A, Van der Linde H, Hermans AN, Lu HR, Towart R *et al*. (2007). In vivo mechanisms precipitating torsades de pointes in a canine model of drug-induced long-QT1 syndrome. *Cardiovasc Res* **76**: 247–256.

Gintant GA, Limberis JT, Mcdermott JS, Wegner CD, Cox BF (2001). The canine Purkinje fiber: an in vitro model system for acquired long QT syndrome and drug-induced arrhythmogenesis. *J Cardiovasc Pharmacol* **37**: 607–618.

Gralinski MR (2003). The dog's role in the preclinical assessment of QT interval prolongation. *Toxicol Pathol* **31** (Suppl.): 11–16.

Guérard NC, Traebert W, Suter W, Dumotier BM (2008). Selective

block of IKs plays a significant role in MAP triangulation induced by IKr block in isolated rabbit heart. *J Pharmacol Toxicol Methods* **58**: 32–40.

Gomoll AW, Bartek MJ (1986). Comparative beta-blocking activities and electrophysiologic actions of racemic sotalol and its optical isomers in anesthetized dogs. *Eur J Pharmacol* **132**: 123–135.

Guo D, Zhao X, Wu Y, Liu T, Kowey PR, Yan GX (2007). L-type calcium current reactivation contributes to arrhythmogenesis associated with action potential triangulation. *J Cardiovasc Electrophysiol* **18**: 196–203.

Gwilt M, Arrowsmith JE, Blackburn KJ, Burges RA, Cross PE, Dalrymple HW *et al*. (1991). UK-68,798: a novel, potent and highly selective class III antiarrhythmic agent which blocks potassium channels in cardiac cells. *J Pharmacol Exp Ther* **256**: 318–324.

Hanson LA, Bass AS, Gintant G, Mittelstadt S, Rampe D, Thomas K (2006). ILSI-HESI cardiovascular safety subcommittee initiative: evaluation of three non-clinical models of QT prolongation. *J Pharmacol Toxicol Methods* **54**: 116–129.

Hohnloser SH, Klingenheben T, Singh BN (1994). Amiodarone-associated proarrhythmic effects. A review with special reference to torsade de pointes tachycardia. *Ann Intern Med* **121**: 529–535.

Hondeghem LM (2007). Relative contributions of TRIaD and QT to proarrhythmia. *J Cardiovasc Electrophysiol* **18**: 655–657.

Hondeghem LM, Carlsson L, Duker G (2001). Instability and triangulation of the action potential predict serious proarrhythmia, but action potential duration prolongation is antiarrhythmic. *Circulation* **103**: 2004–2013.

Hondeghem LM, Hoffmann P (2003). Blinded test in isolated female rabbit heart reliably identifies action potential duration prolongation and proarrhythmic drugs: importance of triangulation, reverse use dependence, and instability. *J Cardiovasc Pharmacol* **41**: 14–24.

Hondeghem LM, Lu HR, Van Rossem K, De Clerck F (2003). Detection of proarrhythmia in the female rabbit heart: blinded validation. *J Cardiovasc Electrophysiol* **14**: 287–294.

Kato R, Ikeda N, Yabek SM, Kannan R, Singh BN (1986). Electrophysiologic effects of the levo- and dextrorotatory isomers of sotalol in isolated cardiac muscle and their in vivo pharmacokinetics. *J Am Coll Cardiol* **7**: 116–125.

Lawrence CL, Bridgland-Taylor MH, Pollard CE, Hammond TG, Valentin JP (2006). A rabbit Langendorff heart proarrhythmia model: predictive value for clinical identification of torsades de pointes. *Br J Pharmacol* **149**: 845–860.

Lathrop DA (1985). Electromechanical characterization of the effects of racemic sotalol and its optical isomers on isolated canine ventricular trabecular muscles and Purkinje strands. *Can J Physiol Pharmacol* **63**: 1506–1512.

Lengyel C, Varró A, Tábori K, Papp JG, Baczkó I (2007). Combined pharmacological block of IKr and IKs increases short-term QT interval variability and provokes torsades de pointes. *Br J Pharmacol* **151**: 941–951.

Li XW, Niu SC, Zhang XP, Lu JY, Bai F, Zhang L *et al*. (2006). Differences of promethazine and terfenadine on ion channels in guinea pig ventricular myocytes. *Chin Med J (Engl)* **119**: 944–947.

Lu HR, Marien R, Saels A, De Clerck F (2001). Species plays an important role in drug-induced prolongation of action potential duration and early afterdepolarizations in isolated Purkinje fibers. *J Cardiovasc Electrophysiol* **12**: 93–102.

Lu HR, Vlaminckx E, Gallacher DJ (2007). Choice of cardiac tissue in vitro plays an important role in assessing the risk of drug-induced cardiac arrhythmias in human: Beyond QT prolongation. *J Pharmacol Toxicol Methods* **57**: 1–8.

Lu HR, Vlaminckx E, Van De Water A, Rohrbacher J, Hermans A, Gallacher DJ (2006). In-vitro experimental models for the risk assessment of antibiotic-induced QT prolongation. *Eur J Pharmacol* **553**: 229–239.

Manley BS, Alexopoulos D, Robinson GJ, Gobbe SM (1986). Subsidiary class III effects on beta blockers? A comparison of atenolol, metoprolol, nadolol, oxprenolol and sotalol. *Cardiovasc Res* **20**: 705–709.

Masumiya H, Saito M, Ito M, Matsuda T, Noguchi K, Iida-Tanaka N *et al*. (2004). Lack of action potential-prolonging effect of terfenadine on rabbit myocardial tissue preparations. *Biol Pharm Bull* **27**: 131–135.

Michael G, Dempster J, Kane KA, Coker SJ (2007). Potentiation of E-4031-induced torsade de pointes by HMR1556 or ATX-II is not predicted by action potential short-term variability or triangulation. *Br J Pharmacol* **152**: 1215–1227.

Michael G, Kane KA, Coker SJ (2008). Adrenaline reveals the torsadogenic effect of combined blockade of potassium channels in anaesthetized pigs. *Br J Pharmacol* **154**: 1414–1426.

Milberg P, Ramtin S, Monnig G, Osada N, Wasmer K, Breithardt G *et al*. (2004). Comparison of the in vitro electrophysiologic and proarrhythmic effects of amiodarone and sotalol in a rabbit model of acute atrioventricular block. *J Cardiovasc Pharmacol* **44**: 278–286.

Ming Z, Nordin C (1995). Terfenadine blocks time-dependent $Ca2^+$, Na^+, and K^+ channels in guinea pig ventricular myocytes. *J Cardiovasc Pharmacol* **26**: 761–769.

Mohammad S, Zhou Z, Gong Q, January CT (1997). Blockage of the HERG human cardiac K+ channel by the gastrointestinal prokinetic agent cisapride. *Am J Physiol* **273**: H2534–H2538.

Obreztchikova MN, Sosunov EA, Plotnikkov A, Anykhovsky EP, Gainullin RZ, Danilo P *et al*. (2003). Developmental changes in IKr and IKs contribute to age-related expression of dofetilide effects on repolarization and proarrhythmia. *Cardiovasc Res* **59**: 339–350.

Omata T, Kasai C, Hashimoto M, Hombo T, Yamamoto K (2005). QT PRODACT: comparison of non-clinical studies for drug-induced delay in ventricular repolarization and their role in safety evaluation in humans. *J Pharmacol Sci* **99**: 531–541.

Quan XQ, Bai R, Liu N, Chen BD, Zhang CT (2007). Increasing gap junction coupling reduces transmural dispersion of repolarization and prevents torsade de pointes in rabbit LQT3 model. *J Cardiovasc Electrophysiol* **18**: 1184–1189.

Poelzing S, Rosenbaum DS (2004). Nature, significance, and mechanisms of electrical heterogeneities in ventricle. *Anat Rec A Discov Mol Cell Evol Biol* **280**: 1010–1017.

Pollard CE, Valentin J-P, Hammond TG (2008). Strategies to reduce the risk of drug-induced QT interval prolongation: a pharmaceutical company perspective. *Br J Pharmacol* **154**: 1538–1543.

Pratt CM, Ruberg S, Morganroth J, Mcnutt B, Woodward J, Harris S *et al*. (1996). Dose-response relation between terfenadine (Seldane) and the QTc interval on the scalar electrocardiogram: distinguishing a drug effect from spontaneous variability. *Am Heart J* **131**: 472–480.

Redfern WS, Carlsson L, Davis AS, Lynch WG, Mackenzie I, Palethorpe S *et al*. (2003). Relationships between preclinical cardiac electrophysiology, clinical QT interval prolongation and torsade de pointes for a broad range of drugs: evidence for a provisional safety margin in drug development. *Cardiovasc Res* **58**: 32–45.

Singh BN (1999). Current antiarrhythmic drugs: an overview of mechanisms of action and potential clinical utility. *J Cardiovasc Electrophysiol* **10**: 283–301.

So PP-S, Backx PH, Dorian P (2008). Slow delayed rectifier K^+ current block by HMR 1556 increases dispersion of repolarization and promotes torsades de pointes in rabbit ventricles. *Br J Pharmacol* (online publication 6 October 2008; doi: 10.1038/bjp.2008.354).

Spitzer KW, Pollard AE, Yang L, Zaniboni M, Cordeiro JM, Huelsing DJ (2006). Cell-to-cell electrical interactions during early and late repolarization. *J Cardiovasc Electrophysiol* **17**: S8–S14.

Stengl M, Ramakers C, Donker DW, Nabar A, Rybin AV, Spätjens RL *et al*. (2006). Temporal patterns of electrical remodeling in canine ventricular hypertrophy: focus on IKs downregulation and blunted beta-adrenergic activation. *Cardiovasc Res* **72**: 90–100.

Szabo G, Szentandrassy N, Biro T, Toth BI, Czifra G, Magyar J *et al*. (2005). Asymmetrical distribution of ion channels in canine and

human left-ventricular wall: epicardium versus midmyocardium. *Pflugers Arch* **450**: 307–316.

Tande PM, Refsum H (1988). Class III antiarrhythmic action linked with positive inotropy: effects of the d- and l-isomer of sotalol on isolated rat atria at threshold and suprathreshold stimulation. *Pharmacol Toxicol* **62**: 272–277.

Terrar DA, Wilson CM, Graham SG, Bryant SM, Heath BM (2007). Comparison of guinea-pig ventricular myocytes and dog Purkinje fibres for in vitro assessment of drug-induced delayed repolarization. *J Pharmacol Toxicol Methods* **56**: 171–185.

Thomsen MB, Matz J, Volders PG, Vos MA (2006). Assessing the proarrhythmic potential of drugs: current status of models and surrogate parameters of torsades de pointes arrhythmias. *Pharmacol Ther* **112**: 150–170.

Thomsen MB, Oros A, Schoenmakers M, Van Opstal JM, Maas JN, Beekman JD *et al*. (2007). Proarrhythmic electrical remodelling is associated with increased beat-to-beat variability of repolarisation. *Cardiovasc Res* **73**: 521–530.

Thomsen MB, Verduyn SC, Stengl M, Beekman JD, De Pater G, Van Opstal J *et al*. (2004). Increased short-term variability of repolarization predicts d-sotalol-induced torsades de pointes in dogs. *Circulation* **110**: 2453–2459.

Volders PG, Sipido KR, Vos MA, Kulcsar A, Verduyn SC, Welliens HJ (1998). Cellular basis of biventricular hypertrophy and arrhythmogenesis in dogs with chronic complete atrioventricular block and acquired torsade de pointes. *Circulation* **98**: 1136–1147.

Volders PG, Stengl M, van Opstal JM, Gerlach U, Spätjens RL, Beekman JD *et al*. (2003). Probing the contribution of IKs to canine ventricular repolarization: key role for beta-adrenergic receptor stimulation. *Circulation* **107**: 2753–2760.

Zaniboni M, Pollard AE, Yang L, Spitzer KW (2000). Beat-to-beat repolarization variability in ventricular myocytes and its suppression by electrical coupling. *Am J Physiol Heart Circ Physiol* **278**: H677–H687.